

Ab-initio simulation of optical-field induced currents in dielectrics

Georg Wachter^{1,*}, Christoph Lemell¹, Joachim Burgdörfer¹,
Shunsuke A. Sato², Xiao-Min Tong^{2,3}, and Kazuhiro Yabana^{2,3}

¹*Institute for Theoretical Physics, Vienna University
of Technology, 1040 Vienna, Austria, EU*

²*Graduate School of Pure and Applied Sciences,
University of Tsukuba, Tsukuba 305-8571, Japan and*

³*Center for Computational Sciences,
University of Tsukuba, Tsukuba 305-8577, Japan*

(Dated: December 3, 2024)

Abstract

We theoretically investigate the generation of ultrafast currents in insulators induced by strong few-cycle laser pulses. Ab-initio simulations based on time-dependent density functional theory give insights into the atomic-scale properties of the induced current signifying a femtosecond-scale insulator-metal transition. We observe the transition from nonlinear polarization currents during the laser pulse at low intensities to tunneling-like excitation into the conduction band at higher laser intensities. At high intensities, the current persists after the conclusion of the laser pulse considered to be the precursor of the dielectric breakdown on the femtosecond scale. We show that the transferred charge sensitively depends on the orientation of the polarization axis relative to the crystal axis suggesting that the induced charge separation reflects the anisotropic electronic structure. We find good agreement with very recent experimental data on the intensity and carrier-envelope phase dependence [1].

PACS numbers: 71.15.Mb, 42.50.Hz, 78.47.J-, 72.20.Ht

The availability of femtosecond laser sources providing wave-form controlled high-intensity pulses has opened up novel opportunities to explore the ultrafast and non-linear response of matter. While experiments with rare-gas targets have provided considerable insight into the real-time motion of electrons within atoms and during the ionization process and ensuing the non-linear optical response in terms of high-harmonic generation [2], the exploration of laser-induced sub-femtosecond processes in the realm of solid-state and surface physics is only at the very beginning [3–6]. Delicate light-field control of electron currents emitted from surfaces, nanostructures, and nanoparticles have been demonstrated [7–11] while experiments with bulk matter have succeeded to monitor the electronic dynamics indirectly through optical signals [12].

Very recently, Schiffrin *et al.* [1] have shown that strong few-cycle laser pulses induce currents and charge separation in large band-gap dielectrics. Their experiment gives direct access to the amount of charge transferred between two electrodes by the laser electric field. In contrast to the electrical current and subsequent electron-avalanche breakdown induced by static fields or picosecond laser pulses [13], the charge transfer observed in [1] results from optical-field induced transient and reversible currents below the destruction threshold. These results suggest that the intense laser field strongly distorts the electronic band structure thereby converting an insulator transiently into a metal on the (sub) femtosecond scale. This picture is supported by first modeling efforts based on semi-classical Bloch equations [14] or independent-particle tight-binding models [1, 15, 16] including macroscopic screening effects [1, 17, 18]. Since all previous approaches are based on mostly one-dimensional phenomenological models, the interrelation between the ultrafast dynamics and the microscopic lattice and electronic structure of the dielectric remains to be understood. Open questions include: Does the current correspond to a nonlinear Maxwellian polarization current leading to a finite polarization after the end of the driving laser pulse? Is the current due to electrons non-adiabatically transferred into the conduction band where transport might continue after the conclusion of the driving laser pulse? Does the relative orientation of the laser polarization and crystallographic axes influence the ultrafast response? What are similarities and differences to pulse-shape sensitive currents emitted from atomic gas targets [19]?

In this Letter, we investigate the origin of optical field-induced currents in bulk insulators on the atomic scale. We present the first fully three-dimensional ab-initio simulations based on time-dependent density functional theory (TDDFT). Our simulations give access to the

dynamics of microscopic quantities including the spatially and time resolved electron density and electrical current density within the unit cell of the material. The simulations thereby provide unprecedented insight into the spatio-temporal structure of the charge dynamics on the atomic length and time scale.

We employ a real-space, real-time formulation of TDDFT [20–24] to simulate the electronic dynamics induced by strong few-cycle laser pulses in α -SiO₂ (α -quartz). Details of the simulation for α -SiO₂ have been reported in [24]. Briefly, we solve the time-dependent Kohn-Sham equations (atomic units used unless stated otherwise)

$$i\partial_t\psi_i(\mathbf{r}, t) = H(\mathbf{r}, t)\psi_i(\mathbf{r}, t) \quad , \quad (1)$$

where the index i runs over the occupied Kohn-Sham orbitals ψ_i with the Hamiltonian

$$H(\mathbf{r}, t) = \frac{1}{2} (-i\nabla + \mathbf{A}(t))^2 + \hat{V}_{\text{ion}} + \int d\mathbf{r}' \frac{n(\mathbf{r}', t)}{|\mathbf{r} - \mathbf{r}'|} + \hat{V}_{\text{XC}}(\mathbf{r}, t) \quad (2)$$

describing the system under the influence of a homogenous time-dependent electric field $\mathbf{F}(t)$ of amplitude \mathbf{F}_0 with a vector potential $\mathbf{A}(t) = -\int_{-\infty}^t \mathbf{F}(t')dt'$ in the velocity gauge and in the transverse geometry [25]. The periodic lattice potential \hat{V}_{ion} is given by norm-conserving pseudopotentials of the Troullier-Martins form [26] representing the ionic cores (O(1s²) and Si(1s²2s²2p⁶)). The valence electron density is given as $n(\mathbf{r}, t) = \sum_i |\psi_i(\mathbf{r}, t)|^2$. For the exchange and correlation potential \hat{V}_{XC} we employ the recently proposed adiabatic Tran-Blaha modified Becke-Johnson meta-GGA functional [27–30] which has been shown to accurately represent the band gap in ground state calculations yielding ~ 9 eV for SiO₂ and moreover a good approximation to the dielectric function at optical frequencies, $\text{Re}(\varepsilon(\omega)) \sim 2.2$ at 800 nm, compared to the experimental value 2.4 [31].

We solve the time-dependent Kohn-Sham equations (Eq. 1) on a Cartesian grid with discretization ~ 0.20 a.u. in laser polarization direction and ~ 0.45 a.u. perpendicular to the polarization direction in a cuboid cell of dimensions $9.28 \times 16.05 \times 10.21$ a.u.³ employing a nine-point stencil for the kinetic energy operator and a Bloch-momentum grid of 4^3 \mathbf{k} -points. The time evolution is performed with a 4th-order Taylor approximation to the Hamiltonian with a time step of 0.02 a.u. including a predictor-corrector step. We analyze the time and space dependent microscopic current density

$$\mathbf{j}(\mathbf{r}, t) = |e| \sum_i \frac{1}{2} [\psi_i^*(\mathbf{r}, t) (-i\nabla + \mathbf{A}(t)) \psi_i(\mathbf{r}, t) + \text{c.c.}] \quad . \quad (3)$$

The macroscopic current density $J(t)$ along the laser polarization direction \mathbf{F}_0 is given by the average of $\mathbf{j}(\mathbf{r}, t)$ over the unit cell with volume Ω

$$J(t) = \frac{1}{\Omega} \int_{\Omega} d\mathbf{r} \mathbf{j}(\mathbf{r}, t) \cdot \mathbf{F}_0 / |\mathbf{F}_0| \quad (4)$$

and the corresponding polarization density is $P(t) = \int_{-\infty}^t J(t') dt'$. $P(t)$ gives the charge transferred per unit area at time t . Accordingly, the macroscopic charge transferred by the laser pulse follows from $P(t > \tau_p)$ after the conclusion of the pulse as

$$Q_L = P(t > \tau_p) \mathcal{A}_{\text{eff}} \quad , \quad (5)$$

where \mathcal{A}_{eff} is the effective surface perpendicular to the laser polarization direction of the target illuminated by the laser.

For a moderate laser intensity of $5 \times 10^{12} \text{W/cm}^2$ where the onset of the non-linear response is expected, the time-dependent polarization density $P(t)$ (Fig. 1) follows approximately adiabatically the applied electric force as expected within linear response ($P(t) \approx (\varepsilon - 1)E(t)$). However, after the pulse is over, the polarization density shows small-scale and fast oscillations. Their dominant oscillation frequency corresponds to the beating frequency between states in the valence and conduction band (period ~ 0.5 fs). The average over these oscillations yields a small but finite sustained polarization density after the pulse, corresponding to a transferred charge density of about 1×10^{-7} electrons per a.u.² (Fig. 1). This transferred charge remains, within the time interval covered by our propagation, constant to a good degree of approximation indicating the absence of any sustained current. The situation changes dramatically for an increased laser intensity of $2 \times 10^{14} \text{W/cm}^2$. During the laser pulse, the polarization density is distorted and phase shifted relative to the laser field. After the pulse has concluded at $t = \tau_p$, the polarization density shows an almost linear decrease pointing to a constant current density flowing after the laser pulse is over. Such a ballistic current will eventually relax due to dissipative processes such as electron-electron, electron-phonon, and impurity scattering on longer time scales (20 to 100 fs) beyond the range of our present simulation. The appearance of quantum beats and a sustained current after the conclusion of the laser pulse qualitatively confirms earlier findings employing one-dimensional models [15, 17]. The beating amplitude is drastically reduced compared to phenomenological models [15] as screening is self-consistently taken into account.

The time-averaged local current density after the laser pulse has concluded, $\mathbf{j}(\mathbf{r}, t > \tau_p)$, gives first insight into the excitation mechanism. For low laser intensity (Fig. 2(a)) it is

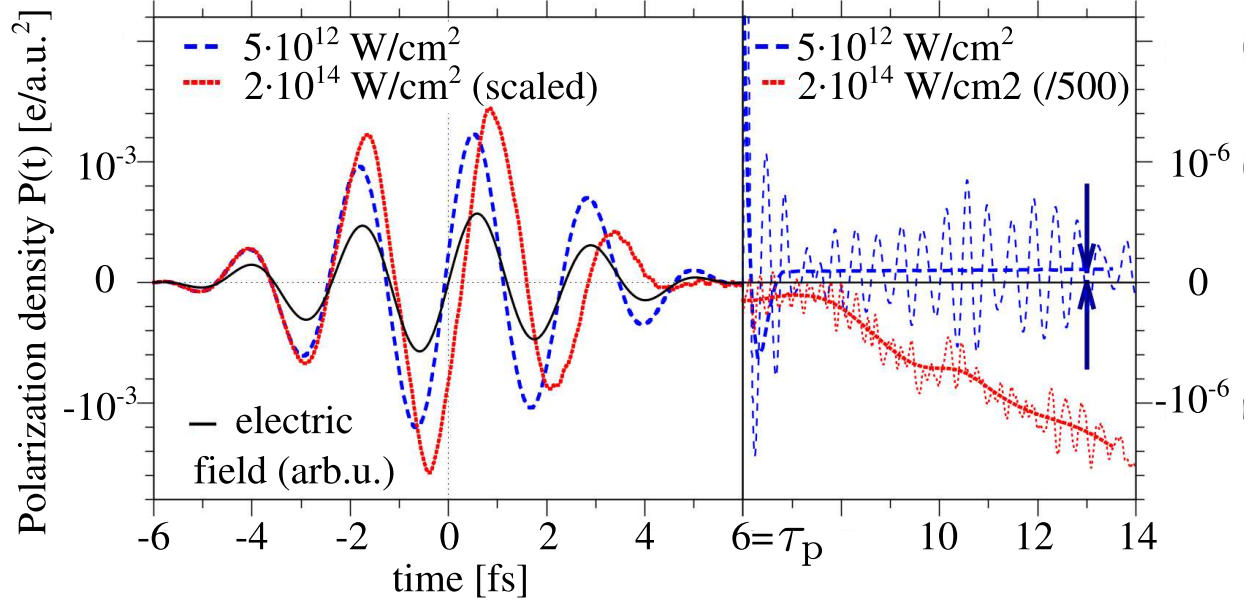


FIG. 1. (Color online) Time-dependent macroscopic polarization density $P(t)$ along the laser polarization direction calculated for two different laser intensities (blue dashed line: 5×10^{12} W/cm² corresponding to a peak field strength of $|\mathbf{F}_0| = 0.012$ a.u., red dotted line: 2×10^{14} W/cm², $P(t)$ scaled by the field amplitude ratio for easy comparison, black solid line: laser field with photon energy 1.7 eV and pulse duration (full width) of $2\tau_p = 12$ fs). Note the change in ordinate scale after the end of the pulse ($\tau_p = 6$ fs, right panel). Temporal averages (thick lines) over fast oscillations (thin lines). The vertical arrows indicate the persisting polarization after the laser pulse.

centered around the O atoms with a slight elongation along the laser polarization direction (in Fig. 2(a)) taken along the \hat{c} axis of the crystal) while the current density near the Si atoms and in the interstitial region is negligible, suggesting that essentially atomic-like orbitals are populated resembling atomic photoexcitation. At the higher laser intensity (Fig. 2(b)) the situation is notably different: the current density distribution extends along the Si-O-Si bond axis and into the interstitial region near the Si atoms indicating laser-induced population of delocalized conduction band levels.

The transition to the excitation regime of a quasi-free current can be visualized by snapshots of the time-dependent current density $\mathbf{j}(\mathbf{r}, t)$ near the extremum of the laser field (Fig. 3(a)). Within the strong field ionization (SFI) model [32] the excitation process is governed by the magnitude of the Keldysh parameter $\gamma = \omega\sqrt{2\Delta}/F_0$ with Δ the gap between

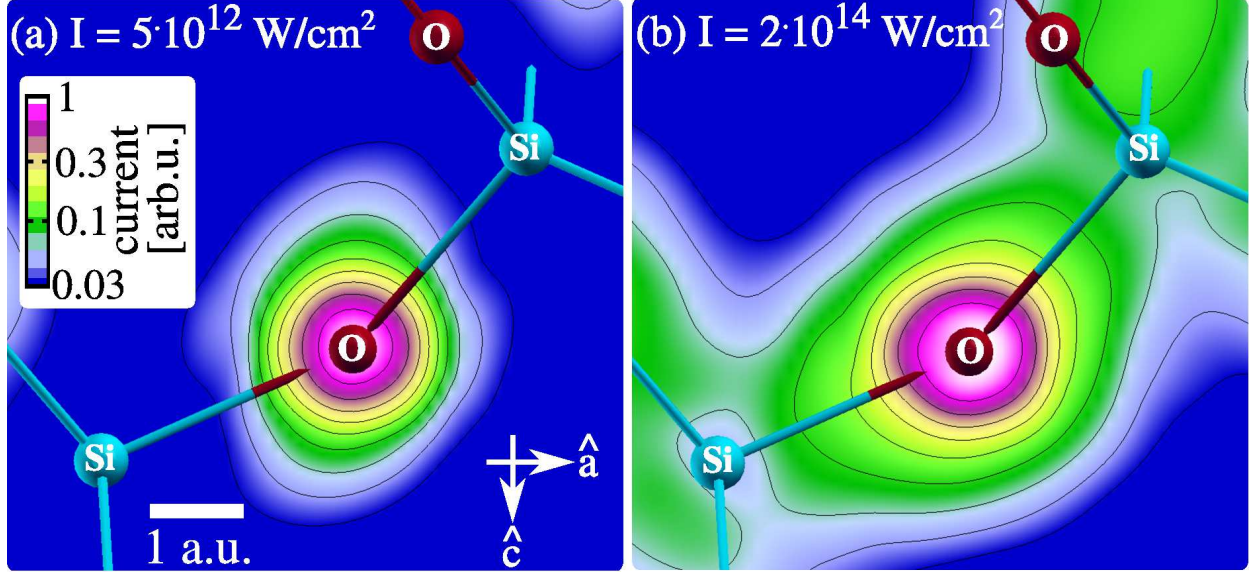


FIG. 2. (Color online) Time-averaged current density $|\mathbf{j}(\mathbf{r}, t > \tau_p)|$ in an \hat{a} - \hat{c} -plane of the trapezohedral SiO_2 lattice where the plane cuts through the O atom of a Si-O-Si bond, the laser is polarized in \hat{c} direction. (a) Laser intensity $5 \times 10^{12} \text{ W/cm}^2$, (b) laser intensity $2 \times 10^{14} \text{ W/cm}^2$.

the valence and conduction bands of the dielectric and F_0 the peak laser field strength. For $\gamma \gg 1$, multi-photon transition dominates while $\gamma \ll 1$ marks the regime of tunnel ionization. Accordingly, at an intensity of $2 \times 10^{14} \text{ W/cm}^2$ the Keldysh parameter for transitions to the conduction band is $\gamma \approx 0.7$, i.e. in the transition regime to tunneling excitation. For an isotropic static potential landscape, the tunneling current is expected to be oriented along the electric force direction exerted by the laser. In the present case of an anisotropic potential with the O-Si bonding direction at a finite angle relative to \mathbf{F}_0 , the current displays a slight tilt (Fig. 3(a)), consistent with the charge transfer to the Si atom and into the interstitial region. This directionality of the tunneling process in real space leaves its marks also in momentum space. For low laser intensities, coupling to the conduction band is weak and almost fully reversible. Moreover, \mathbf{k} -points oriented parallel and anti-parallel to the laser amplitude are nearly equally populated after the laser pulse (Fig. 3(b)) resulting in a vanishing free current. Transitions to the conduction band set in when the laser intensity surpasses the value where tunneling excitation occurs. The latter can be estimated from the field strength F_c where the electrostatic potential difference between the O and the Si site (distance $d_{\text{O-Si}} = 3.04 \text{ a.u.}$) reaches the order of magnitude of the excitation gap, $F_c d_{\text{O-Si}} \approx \Delta$. The resulting population of the conduction band states after the conclusion of

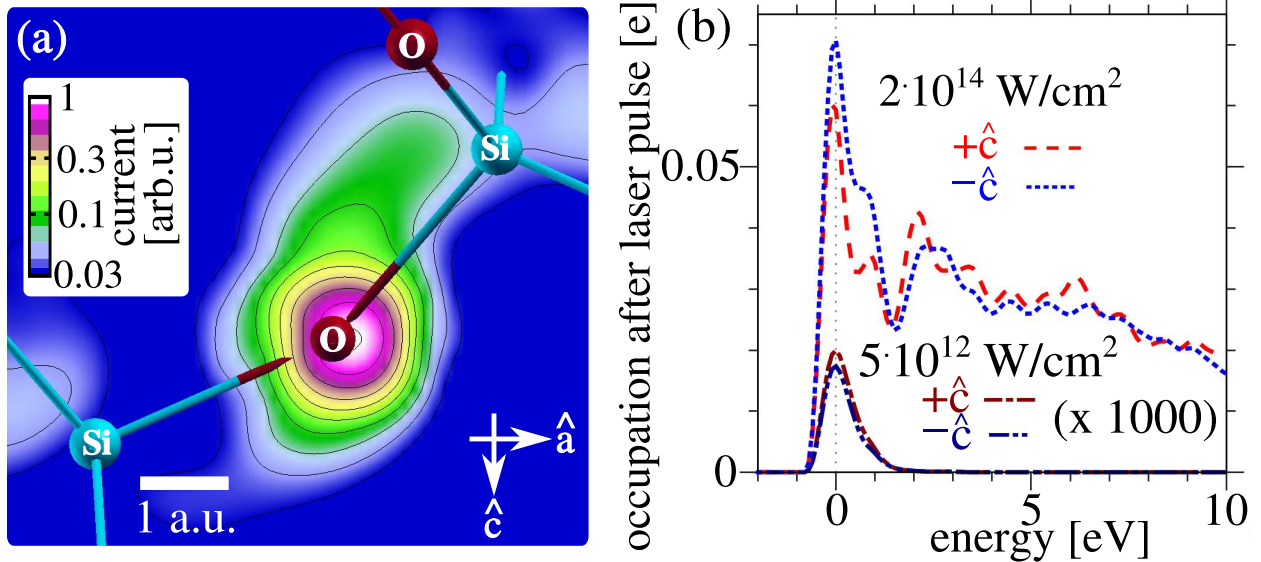


FIG. 3. (Color online) (a) Snapshot of the current density for laser intensity $2 \times 10^{14} \text{ W/cm}^2$ taken near a laser field extremum at simulation time $t \approx -0.5 \text{ fs}$ in Fig. 1. The electric field, oriented along the \hat{c} -axis, induces tunneling between neighboring atoms. (b) Occupation of conduction band states with positive (red lines) and negative (blue lines) \mathbf{k} -vectors with respect to the laser polarization direction \hat{c} for a few-cycle pulse with laser intensities of $5 \times 10^{12} \text{ W/cm}^2$ (lower graphs, magnified by a factor of 1000) and $2 \times 10^{14} \text{ W/cm}^2$ (upper graphs).

the laser pulse is orders of magnitude larger, extends to higher energies, and shows energy-dependent forward-backward asymmetries as a result of tunneling and subsequent evolution (Fig. 3(b)).

The present simulations can be compared with the first experimental data [1]. A comparison on an absolute scale for Q_L (Eq. 5) would require the knowledge of the effective surface area \mathcal{A}_{eff} of the crystal that is illuminated by the laser which is difficult to determine experimentally. We choose \mathcal{A}_{eff} to match the experimental value of $Q_L = 0.6 \text{ A fs}$ at an intensity of $5 \times 10^{13} \text{ W/cm}^2$ yielding a value $\mathcal{A}_{\text{eff}} = 8.7 \times 10^{-14} \text{ m}^2$. Keeping this scaling factor fixed we find excellent agreement over more than two orders of magnitude for Q_L (Fig. 4(a)) without any adjustable parameters. The step rise over more than two orders of magnitude clearly indicates the transition from a reversible non-linear bound polarization current to the excitation of a quasi-free current.

Moreover the experiment [1] has also demonstrated that for a wave-form controlled few-cycle pulse, exquisite light-field control translates into control over the charge transfer. In

particular, Q_L varies sinusoidally with the carrier-envelope phase ϕ_{CE} of the few-cycle pulse (Fig. 4(b)) clearly showing that the field amplitude rather than the intensity is the parameter governing the charge transfer. We find excellent agreement with the experimental ϕ_{CE} dependence for a laser intensity of 5×10^{13} W/cm² ($F_0 = 1.7$ V/Å, Fig. 4(b)). Further, our simulations predict a pronounced change of the carrier-envelope phase dependence with increasing intensity. Observation of the effect will require single crystals with well-defined orientation of the crystallographic axis relative to the laser polarization rather than fused silica targets used in the experiment [1].

We investigate the influence of the anisotropic electronic structure on the transferred charge by comparing simulations with laser polarization along the \hat{a} and \hat{c} axis of the crystal. We find that the dependence of Q_L on both the laser intensity and on the carrier-envelope phase varies with orientation of laser polarization relative to the crystallographic axis in the high-field regime ($I \approx 10^{14}$ W/cm², Fig. 4). Most notably, we observe a pronounced shift by $\approx \pi/4$ in Q_L , $Q_L(\hat{a}, \phi_{CE}) \approx Q_L(\hat{c}, \phi_{CE} + \pi/4)$ (Fig. 4(b)). While the experiment [1] was designed to be sensitive only to the ϕ_{CE} -dependent part of the current and transferred charge, we find an additional unexpected ϕ_{CE} independent contribution to Q_L when the laser polarization is aligned along the \hat{a} axis (Fig. 4(b)). We trace its origin to the broken inversion symmetry along the \hat{a} axis ($\hat{a} \rightarrow -\hat{a}$) of the SiO₂ crystal (see inset Fig. 4(a)). Unlike for the high-symmetry \hat{c} axis, this leads to an average net charge transfer by a few-cycle pulse. Consequently, our simulation predicts that charge transfer in dielectrics induced by ultrafast pulses is possible even without the need for a CE-phase stabilized laser.

The present simulation provides a simple and transparent picture of the current and charge transfer dynamics. At very low laser intensity, well within the linear response regime ($I \leq 10^{12}$ W/cm²), neither a net current nor a charge displacement is induced. With increasing laser intensity, nonlinear effects become important. Starting from about 5×10^{12} W/cm², our simulations show that a finite amount of charge is transferred by nonlinear polarization currents during the laser pulse but no significant quasi-free current flows after the pulse, i.e. these polarization currents are almost completely reversible. Associating these currents with a field-induced AC conductivity $\sigma(\omega_L)$ at carrier frequency ω_L ,

$$J(t) = \sigma(\omega_L)F(t) \quad , \quad (6)$$

the non-linear process of the charge displacement can be viewed as a reversible (sub)-

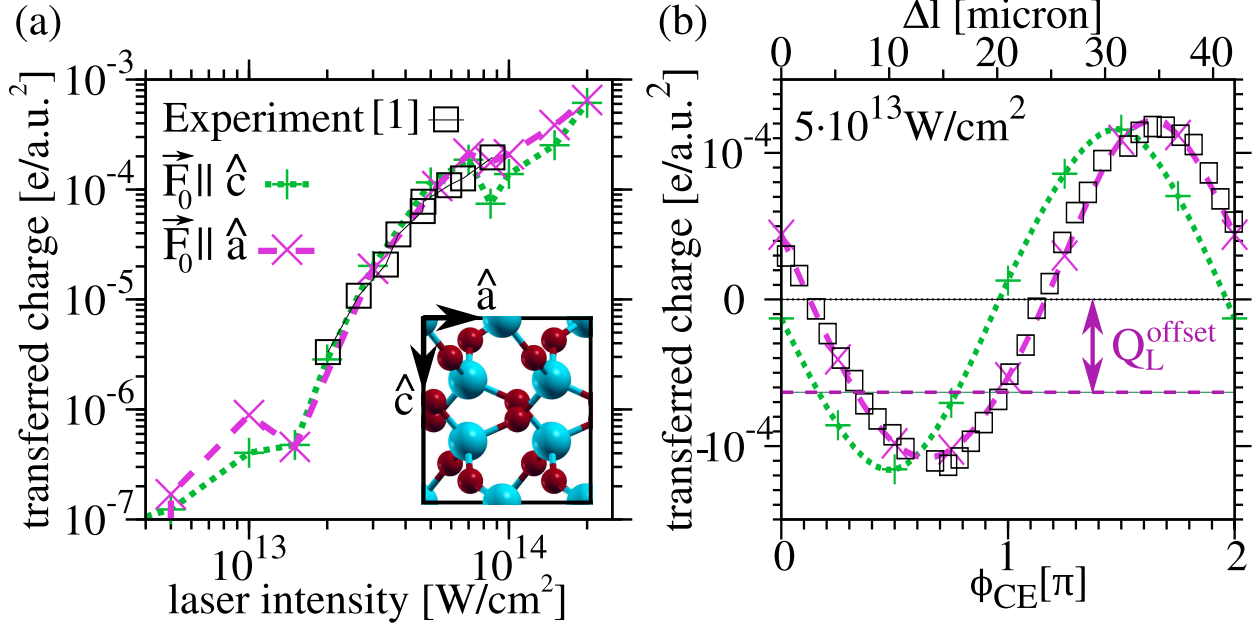


FIG. 4. (Color online) Laser-induced charge transfer Q_L as a function of laser intensity in SiO₂ for photon energy 1.7 eV and pulse length 4.3 fs (FWHM intensity). Green crosses: laser polarized in \hat{c} direction, purple X: laser polarized in \hat{a} direction, black squares: experimental data [1]. (a) Intensity dependence of the ϕ_{CE} -maximized transferred charge, experimental data for an amorphous target. Inset: Projection of the SiO₂ lattice structure onto the \hat{a} - \hat{c} -plane. (b) Carrier-envelope dependence at fixed intensity $5 \times 10^{13} \text{ W}/\text{cm}^2$ where in the simulation ϕ_{CE} is related to the vector potential as $A(t) \propto -\cos(\omega t + \phi_{\text{CE}})$. Experimental data for a single crystal irradiated with polarization direction perpendicular to the \hat{c} axis are plotted against the change Δl in the propagation length through a fused silica wedge. For polarization along \hat{a} , the simulation gives an additional ϕ_{CE} -independent offset shown by the horizontal dashed line.

femtosecond scale insulator to “metal” transition where $\sigma(\omega_L)$ increases by more than 20 orders of magnitude. The character of the field-induced currents changes significantly once the laser intensity is sufficiently high such that a substantial amount of electrons are non-adiabatically excited into the conduction band by tunneling excitation. The onset of a ballistic current in the material after the laser pulse is over is accompanied by a delocalized current density over the unit cell. This marks the precursor of dielectric breakdown for longer pulses. A finite conductivity, i.e. a transition from a femtosecond ballistic current to a dissipative current will be established only on longer time scales (~ 20 fs as estimated from mobility data [33–35]) by dissipative processes such as electron-electron and electron-phonon

scattering. In our simulation, the transition from nonlinear polarization to the regime where quasi-free ballistic electron currents dominate occurs at a laser intensity of about 5×10^{13} W/cm². We find the amount of charge transferred is influenced by the intensity, pulse shape, and polarization direction of the laser pulse in the unit cell, indicating that the charge separation depends sensitively on the details of the potential landscape and bond structure.

The present results suggest opportunities for future investigations of the non-equilibrium electron dynamics on the femtosecond scale, in particular the transition regime from ballistic to dissipative electron transport in a pump-probe setting, possibly employing an optical read-out. Other promising directions include novel information on the anisotropic nonlinear response and on electronic defects such as color centers in wide-bandgap insulators, most notably alkali halides.

Helpful discussions with V. Yakovlev, M. Ivanov, and M. Stockman are gratefully acknowledged. This work was supported by the FWF (Austria), SFB-041 ViCoM, SFB-049 Next Lite, and P21141-N16. G.W. thanks the International Max Planck Research School of Advanced Photon Science for financial support. X.-M.T. was supported by a Grant-in-Aid for Scientific Research (C24540421) from the Japan Society for the Promotion of Science. K.Y. acknowledges support by the Grants-in-Aid for Scientific Research Nos. 23340113 and 25104702. Calculations were performed using the Vienna Scientific Cluster (VSC) and the supercomputer at the Institute of Solid State Physics, University of Tokyo.

REFERENCES

-
- * georg.wachter@tuwien.ac.at
- [1] A. Schiffrin, T. Paasch-Colberg, N. Karpowicz, V. Apalkov, D. Gerster, S. Muhlbrandt, M. Korbman, J. Reichert, M. Schultze, S. Holzner, J. V. Barth, R. Kienberger, R. Ernstorfer, V. S. Yakovlev, M. I. Stockman, and F. Krausz, *Nature* **493**, 70 (2013).
 - [2] F. Krausz and M. Ivanov, *Reviews of Modern Physics* **81**, 163 (2009).
 - [3] A. L. Cavalieri, N. Muller, T. Uphues, V. S. Yakovlev, A. Baltuska, B. Horvath, B. Schmidt, L. Blumel, R. Holzwarth, S. Hendel, M. Drescher, U. Kleineberg, P. M. Echenique, R. Kienberger, F. Krausz, and U. Heinzmann, *Nature* **449**, 1029 (2007).

- [4] M. Gertszov, H. Jean-Ruel, P. Rajeev, D. Klug, D. Rayner, and P. Corkum, *Physical Review Letters* **101** (2008).
- [5] M. Gertszov, M. Spanner, D. M. Rayner, and P. B. Corkum, *Journal of Physics B: Atomic, Molecular and Optical Physics* **43**, 131002 (2010).
- [6] S. Ghimire, A. D. DiChiara, E. Sistrunk, P. Agostini, L. F. DiMauro, and D. A. Reis, *Nat Phys* **7**, 138 (2011).
- [7] C. Lemell, X. M. Tong, F. Krausz, and J. Burgdörfer, *Physical Review Letters* **90**, 076403 (2003).
- [8] P. Dombi, A. Apolonski, C. Lemell, G. G. Paulus, M. Kakehata, R. Holzwarth, T. Udem, K. Torizuka, J. Burgdörfer, T. W. Hänsch, and F. Krausz, *New Journal of Physics* **6**, 39 (2004).
- [9] M. Krüger, M. Schenk, and P. Hommelhoff, *Nature* **475**, 78 (2011).
- [10] G. Wachter, C. Lemell, J. Burgdörfer, M. Schenk, M. Krüger, and P. Hommelhoff, *Physical Review B* **86**, 035402 (2012).
- [11] S. Zherebtsov, T. Fennel, J. Plenge, E. Antonsson, I. Znakovskaya, A. Wirth, O. Herrwerth, F. Suszmann, C. Peltz, I. Ahmad, S. A. Trushin, V. Pervak, S. Karsch, M. J. J. Vrakking, B. Langer, C. Graf, M. I. Stockman, F. Krausz, E. Ruhl, and M. F. Kling, *Nat Phys* **7**, 656 (2011).
- [12] A. V. Mitrofanov, A. J. Verhoef, E. E. Serebryannikov, J. Lumeau, L. Glebov, A. M. Zheltikov, and A. Baltuška, *Physical Review Letters* **106**, 147401 (2011).
- [13] M. Sparks, D. L. Mills, R. Warren, T. Holstein, A. A. Maradudin, L. J. Sham, E. Loh, and D. F. King, *Physical Review B* **24**, 3519 (1981).
- [14] P. Földi, M. G. Benedict, and V. S. Yakovlev, *New Journal of Physics* **15**, 063019 (2013).
- [15] M. Korbman, S. Y. Kruchinin, and V. S. Yakovlev, *New Journal of Physics* **15**, 013006 (2013).
- [16] P. G. Hawkins and M. Y. Ivanov, *Physical Review A* **87** (2013).
- [17] Kruchinin, M. Korbman, and V. S. Yakovlev, *Physical Review B* **87**, 115201 (2013).
- [18] V. Apalkov and M. I. Stockman, *Physical Review B* **86**, 165118 (2012).
- [19] D. B. Milošević, G. G. Paulus, D. Bauer, and W. Becker, *Journal of Physics B: Atomic, Molecular and Optical Physics* **39**, R203 (2006).
- [20] K. Yabana and G. F. Bertsch, *Physical Review B* **54**, 4484 (1996).

- [21] G. F. Bertsch, J. I. Iwata, A. Rubio, and K. Yabana, *Physical Review B* **62**, 7998 (2000).
- [22] G. Onida and A. Rubio, *Reviews of Modern Physics* **74**, 601 (2002).
- [23] M. A. L. Marques and E. K. U. Gross, *Annual Review of Physical Chemistry* **55**, 427 (2004).
- [24] T. Otake, K. Yabana, and J. I. Iwata, *Journal of Physics: Condensed Matter* **21**, 064224 (2009).
- [25] K. Yabana, T. Sugiyama, Y. Shinohara, T. Otake, and G. F. Bertsch, *Physical Review B* **85**, 045134 (2012).
- [26] N. Troullier and J. L. Martins, *Physical Review B* **43**, 1993 (1991).
- [27] F. Tran and P. Blaha, *Physical Review Letters* **102**, 226401 (2009).
- [28] D. Koller, F. Tran, and P. Blaha, *Physical Review B* **83**, 195134 (2011).
- [29] D. Koller, F. Tran, and P. Blaha, *Physical Review B* **85**, 155109 (2012).
- [30] V. U. Nazarov and G. Vignale, *Physical Review Letters* **107**, 216402 (2011).
- [31] H. R. Philipp, *Solid State Communications* **4**, 73 (1966).
- [32] L. V. Keldysh, *Soviet Physics JETP* **20**, 1307 (1965).
- [33] R. Williams, *Physical Review* **140**, A569 (1965).
- [34] A. Goodman, *Physical Review* **164**, 1145 (1967).
- [35] R. Hughes, *Physical Review Letters* **30**, 1333 (1973).